

Ti-based reference electrodes for inline implementation into Lithium-ion pouch cells

Ahmed, Z., Roberts, A. & Amietszajew, T.

Published PDF deposited in Coventry University's Repository

Original citation:

Ahmed, Z, Roberts, A & Amietszajew, T 2021, 'Ti-based reference electrodes for inline implementation into Lithium-ion pouch cells', Energy Technology, vol. (In-Press), 2100602.

<https://dx.doi.org/10.1002/ente.202100602>

DOI 10.1002/ente.202100602

ESSN 2194-4296

Publisher: Wiley-VCH Verlag

This is an open access article under the terms of the Creative Commons Attribution License, which permits use, distribution and reproduction in any medium, provided the original work is properly cited.

Ti-Based Reference Electrodes for Inline Implementation into Lithium-Ion Pouch Cells

Zahoor Ahmed, Alexander J. Roberts, and Tazdin Amietszajew*

Despite growing demand for Li-ion batteries in the portable, industrial, and electric vehicle markets, the performance and safety monitoring of these state-of-the-art rechargeable cells is quite limited, relying on conventional full-cell measurements with in situ reference electrode technologies lagging behind in application. Herein, for the first time a long-term (>2000 h) stable Ti-based reference electrode is reported, and a new design enabling impact-free implementation into pouch. The methodology can also be used with other reference electrode materials. Various electrochemical characterization techniques are used to verify the usability and stability of the developed reference electrode, in turn enabling monitoring of individual electrode cycling performance and open circuit potential (OCP) via the galvanostatic intermittent titration technique (GITT) and differential capacity analysis. The findings offer a potential way of incorporating stable in situ reference electrodes into current and future generations of lithium-ion batteries.

Although the power and energy density of batteries have increased, diagnostics methods are lagging behind. Battery management systems rely on the occasional thermocouple and full-cell potential, with very limited knowledge of the anode and cathode state. Reference electrodes (REs) address this issue by enabling insight into per-electrode processes of Li-ion cells. Despite significant research in the field of energy storage over several decades, a reliable, user-friendly, and artifact-free commercial cell configuration containing a chemically stable reference electrode is far from being widely available,^[3] as to the best of our knowledge no currently available commercial Li-ion batteries are equipped with a dedicated reference electrode. This limits the optimization and monitoring capabilities, and leads to the

1. Introduction


Energy storage devices, such as batteries, are necessary aspects of modern life.^[1] A wide range of industries and fields such as personal computing, aerospace technology, and transportation are highly dependent on access to reliable, uninterrupted power supplies, which are most conveniently provided using lithium-ion battery devices. Lithium-ion batteries have been widely adopted due to their advantages, such as high energy density, large capacity, low self-discharge, and high output potential, creating an area of major interest both in academia and industry.^[2] As such a significant amount of research is focused on improving the cells' performance based on active materials, optimized designs, and reliable diagnostics, which gives rise to variation in batteries' capacity and power output.

black-box problem where we only know input and output, without understanding the internal behavior, because information on limiting processes and individual cell components cannot be obtained.^[4]

Implementation of the REs in small lab-scale cells is understood to be relatively straightforward; however, this is not the case for larger or commercially relevant batteries. Although RE implementation attempts into pouch and cylindrical cells have been reported,^[3] they have yet to be feasibly applied to commercial cells during manufacture, which is mainly due to the manufacturing process, as well as performance and safety constraints. Impact on the cells' operation is often omitted, and introducing reference electrodes into Li-ion cells most often requires significant modifications postproduction,^[5] which changes the system in question, impacting cell operation and safety. In addition, if these modifications are performed after the cell production, even if conducted in an inert atmosphere or a dry room, they can lead to cell damage or even short circuiting, which could eventually lead to catastrophic cell failure.^[4] To be applicable in realistic or even commercially relevant batteries, the extent of required modifications has to be minimized. Previously, we have reported successfully deploying flexible substrate thermistors for monitoring of the temperature distribution inside lithium-ion cells.^[6] Building on the previous experience,^[6–9] we aim to devise a compact component that enables relatively simple implementation into pouch-cell systems with stable reference electrodes.^[10–12]

Standard reference electrodes work on the principle of maintaining a stable equilibrium potential by controlling the concentration of the various reacting chemical species at the electrode/

Z. Ahmed, A. J. Roberts, T. Amietszajew
Institute for Clean Growth & Future Mobility
Coventry University
Coventry CV1 5FB, UK
E-mail: Taz.Amietszajew@coventry.ac.uk

 The ORCID identification number(s) for the author(s) of this article can be found under <https://doi.org/10.1002/ente.202100602>.

© 2021 The Authors. Energy Technology published by Wiley-VCH GmbH. This is an open access article under the terms of the Creative Commons Attribution License, which permits use, distribution and reproduction in any medium, provided the original work is properly cited.

DOI: 10.1002/ente.202100602

electrolyte interface.^[13] A good reference electrode is characterized by nonpolarizability, reproducibility, and long-term stability. However, application of standard REs is always challenging in geometrically constrained nonaqueous systems, where quasi-reference electrodes have to be deployed instead. As such, not having a controlled concentration of a common anion or cation component in the adjacent phases, thermodynamic equilibrium is difficult to achieve. Quasi-references have a number of advantages, however, because they can be immersed directly into the electrolyte and there is no risk of contamination with solvent molecules a standard reference electrode might transfer, enabling them to be deployed inside lithium-ion cells.^[14] Li metal is the most commonly used material as the RE for Li-ion cells; however, it is far from ideal due to the irreversibility of its reactions and the varying influence of different electrolytes on the nature of the passivation layer on the Li surface.

To address these issues, we evaluated a number of Ti-based reference electrode materials—Ti wire, TiO₂ (anatase), and lithium titanate (LTO). Indeed, TiO₂ anatase phase selection was made due to its high thermal stability.^[15–18] A number of electrochemical methods have been utilized to showcase the usefulness of a referenced system while also evaluating its stability. These techniques have included cyclic voltammetry (CV), galvanostatic charge–discharge (GCD), galvanostatic intermittent titration technique (GITT) used to calculate the open circuit potential (OCP) of pouch cells, differential capacity curves (dQ/dV), Coulombic efficiency (CE), and cycling performance.

In this work, we devise a reference electrode design compatible with various pouch-cell formats, and use it to evaluate the chosen reference electrode materials by integrating into commercially available pouch cells. The reference element insertion was accomplished during the standard cell production procedure utilizing pilot line production facilities. This allows for greater insight into the internal cell electrochemistry feasible for commercially relevant Li-ion cell formats. Finally, we evaluate the stability of the deployed reference electrodes over a long period of time and cycling, recommending a stable and straightforward option for a plug-and-play reference electrode solution. The aim of this work was to validate our flat-profile reference electrode in a simulated real-world production setting and subsequently evaluate a number of reference electrode materials with the aim of finding a long-term stable solution.

2. Experimental Section

2.1. Reference Electrode Sensor Fabrication

Two types of reference electrodes were used. For in-pouch insertion, reference electrode sensors were fabricated using flexible printed circuit board (PCB) manufacturing technology, using a 25 μm flexible polyimide (Kapton) as a substrate, a material already existing inside most commercial Li-ion cells.^[19] Such a design allows for implementation during cell production, as detailed in a subsequent section of this article, minimizing the extent of modification. A gold-coated copper pad acts as a current collector, enabling a number of material options to be evaluated and applied as a reference electrode. **Figure 1A** show the design of the reference electrode element. This does not

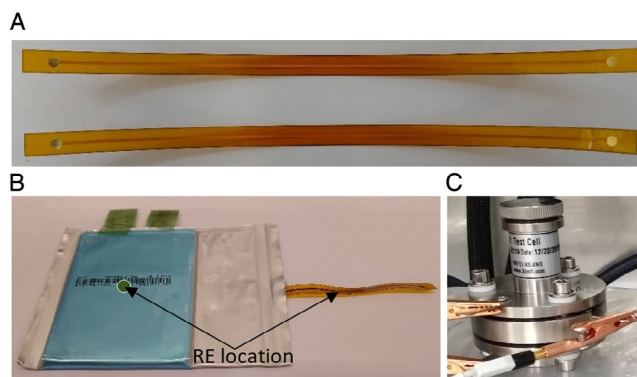


Figure 1. A) RE strip for in-pouch insertion, B) complete pouch cell after final seal, and C) an assembled split cell.

apply to naked metal (Ti, Li) materials, which were used as-is, cleaned, and inserted into pouch cells or split cells for testing.

To protect the previously described element and ensure the long-lasting functionality of the assembly, a 5 μm conformal coating of parylene was deposited prior to embedding into the pouch cells. Parylene barrier properties are known and used by other researchers.^[19,20] To avoid coating of elements exposed by design—connectors, copper pads—a layer of masking tape was applied in relevant places before the coating procedure.

Electrode inks were prepared for the LTO and TiO₂ materials and drop cast using the reference strips shown in Figure 1A at one end and also for split-cell testing were cast onto battery grade aluminum foil using a draw-down coater and doctors blade. These were then dried at 80 °C under vacuum for 12 h. The LTO ink was produced through mixing via a disperser mixer in 1-methyl-2-pyrrolidone (NMP) solvent with C65 carbon black (Imerys, UK) and PvdF (Solvay, France) in the ratio 90:5:5. The TiO₂ ink was also produced through disperser mixing in water solvent of TiO₂, C65, carboxymethyl cellulose (CMC), and styrene butadiene rubber (SBR) in the ratio 90:5:2.5:2.5. The loading weight of the active material was 2 mg cm⁻². The electrode discs of 15 mm diameter were punched and again dried at 80 °C in a vacuum oven for 4 h to remove the traces of moisture present. Finally, electrodes were transferred and used in an argon-filled glove box.

After insertion into the pouch, in case of LTO the reference electrode material needed to be conditioned in situ after the cell formation. This was achieved by running a standard formation procedure, followed by charging the RE to half-capacity to ensure midplateau potential (1.55 V vs Li/Li⁺ for LTO).^[21] Due to the miniature size of the reference electrode element, the amount of current transfer required is negligible in relation to the full cell. The TiO₂ RE however does not require this step as it can be readily used after insertion, making it a more optimal choice from the cell production complexity and time point of view.

For the lithium RE used as a benchmark, a 0.6 mm thick lithium foil was cut into 2 mm × 60 mm and physically attached to a copper wire. This was subsequently wrapped using a portion of separator sheet reclaimed from the same cell model. All parts were fixed for electrode alignment using battery-grade adhesive Kapton tapes. The sandwiched assembly was then inserted in the pouch, ready for electrolyte filling and sealing.

2.2. Electrochemical Cell Assembly

The pouch cells used for this study were Li-Fun Technology lithium-ion dry (without electrolyte) “575166” cells (51 mm × 66 mm), with NMC532 cathodes and graphite anodes in a wound configuration. To evaluate the real-world viability of the proposed RE embedding methodology, the cell build process was finalized following battery pilot line production measures. Reference electrodes were inserted into the middle of the dry pouches (the location is shown in Figure 1B) immediately before the electrolyte-filling step. The cells were then injected with the electrolyte—1 M solution of LiPF₆ mix in ethylene carbonate (EC):ethyl methyl carbonate (EMC) 3:7 + 10% fluorinated ethyl carbonate (FEC) (Solvionic)—vacuum sealed, and left to soak for 24 h at 25 °C. After completion of the assembly, the cells were subjected to a formation procedure,^[19,22] shown in Figure S1, Supporting Information. Complete cells are shown in Figure 1B. In parallel, three-electrode split cells were used with lithium metal counter and reference electrodes (Figure 1C).

2.3. Electrochemical Protocols

To evaluate the cells' behavior during a typical operation, standard cycling procedure of constant current followed by constant-voltage charge and constant-current discharge was performed. All the cells were cycled between 2.5 and 4.2 V with a VMP3 multichannel potentiostat (Bio-Logic Science Instruments) using a current of 240 mA and a 60 mA cutoff limit for the constant-voltage step. For convention, the cathode potential is referred to as working electrode V_{WE} (WE-RE), anode potential as counter electrode V_{CE} (CE-RE), and full-cell potential as V_{Cell} (WE-CE). All tests were performed in a temperature-controlled chamber (Binder) at 25 °C.

CV was performed using split-three electrodes cells on Ti wire, TiO₂, and LTO at a scan rate of 0.5 mV s⁻¹ with the potential window for each test selected between 0.5 and 3.0 V within each material stability window. The split cells were assembled inside an argon-filled glove box and transferred to the temperature-controlled chamber for testing.

The open circuit voltage (OCV) calculated from GITT is referred to as OCP-GITT. It was used to further evaluate the

behavior and stability of the materials used. A 0.2C current pulse was applied for 5 min for 100 pulses in the voltage range of OCP 4.2 V. The rest period between pulses was 60 min during charge and discharge for the GITT experiment. Differential capacities as a function of voltage (dQ/dV) were also analyzed for the pouch cells, derived from galvanostatic cycling. A Savitzky–Golay filter using the Origin lab analysis package was performed on the obtained differential capacity curves.^[23,24]

3. Results and Discussion

3.1. RE Integration

The herein-devised reference electrodes were successfully implemented during the cell-filling and sealing steps, later providing readings discussed in the subsequent sections. The final built cells are shown in Figure 1B. The subsequent LTO reference electrode formation is shown in Figure S1B, Supporting Information. The cells' capacity retention compared to that of standard cells without an inserted electrode was used to verify the impact of the sensor and is discussed in a subsequent section.

3.2. Electrochemical Measurements and Stability Monitoring

CV was recorded between 0.5 and 3 V (vs Li/Li⁺) to better understand the various electrochemical processes that occur during oxidation/reduction on the Ti wire, TiO₂, and LTO crystal lattice. Figure 2 shows the CV curves at 0.2 mV s⁻¹ for REs of Ti wire, TiO₂, and LTO in Li cells. It is observed in the CV that both samples show one pair of anodic/cathodic peaks at around 2.1 and 1.7 V for TiO₂^[25–27] and 2.0 and 1.1 V for LTO against Li/Li⁺, with an average peak of 1.55 V, respectively.^[28,29] This can be attributed to the Ti⁺³/Ti⁺⁴ redox reaction, and also related to the removal of Li⁺ from different lithium lattice sites in the structure that activate at various potentials and energies.

It is observed in Figure 2A,B that anodic/cathodic peak intensity is higher for TiO₂ and LTO during the first cycle. Similar behavior is observed for Ti wire in Figure 2C during cathodic scan, which decreases significantly during the second cycle. First, it can be attributed to the initial surface effects such as the electrolyte interface formation (SEI) and further intercalation

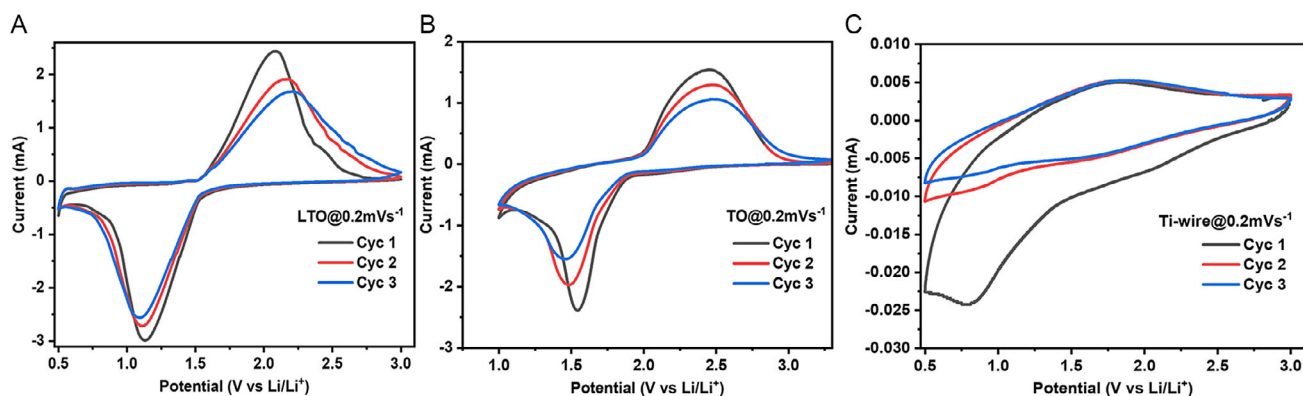


Figure 2. CV curves of A) LTO, B) TiO₂, and C) Ti wire at a scan rate of 0.2 mV s⁻¹.

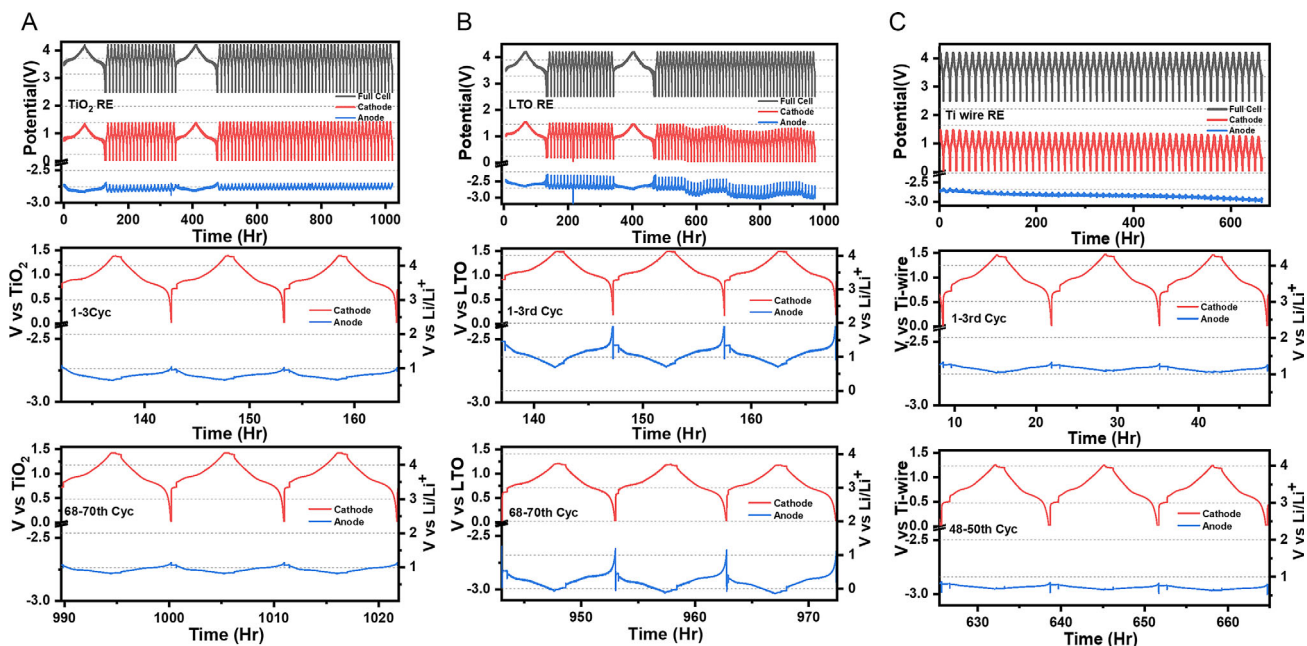


Figure 3. Anode, cathode, and full-cell potential profiles of a pouch cell fitted with an RE. It represents 200 mA (C/5) cycling rate. A) TiO_2 , B) LTO, and C) Ti wire. The RE element was subsequently monitored over the course of 6 weeks, providing stable readings for TiO_2 .

of Li^+ into the structure.^[25] This also suggests that only from the second cycle can we observe a full transformation of the anatase TiO_2 to the Li_xTiO_2 phase.^[26] These measurements conform to the theory of two-phase and irreversible transformation after the second peak from TiO_2 to LiTiO_2 .^[30,31]

The potential profiles for cathode, anode, and full cell with respect to the Ti-wire, TiO_2 , LTO, and Li REs obtained during prolonged cycling are shown in **Figure 3**. The stability of the readings obtained indicate long-term functionality of the reference electrode element. TiO_2 displays long-term stability over 1000 h of 0.2 C cycling in **Figure 3A**, compared to LTO in **Figure 3B**, which shows worse reversibility and experiences sudden reading shifts around the 550 h mark. The Ti-wire reference potential for both the cathode and anode shows complete irreversibility and drift in potential after the tenth cycle until the end of testing, as shown in **Figure 3**.

As previously mentioned, TiO_2 is a preferred option due to no additional formation step being required (unlike for LTO), minimizing the complexity and preparation time required, while it is also safer than pure lithium metal when used as a reference electrode. For comparison, a Li strip as RE in the same setup is shown in **Figure S2**, Supporting Information. Finally, pristine pouch cells without an RE were also tested to provide a baseline for comparison and no significant deviation in the cycling behavior was observed (shown in **Figure S3**, Supporting Information).

Following the promising stability of the TiO_2 reference, it was further cycled, bringing the test period to over 2000 h. Cell potential profiles for the cathode, anode, and full cell with respect to the TiO_2 RE over that extended test period is shown in **Figure S4**, Supporting Information. A good reproducibility of the potential plots for the working and counter electrode was observed during the subsequent cycles.

Long-term stability was further assessed over a 200 h rest period. It was observed that TiO_2 readings remain stable after more than 200 h, with less than 10 mV variation over the OCP time span. In contrast, lithiated LTO and Ti wire shows relatively poor stability, having amounted to more than 20 and 40 mV respectively of the initial potential drift over the test span.

GITT-OCP charge–discharge profiles of the NMC cathode and graphite anode as measured using TiO_2 , LTO, and Ti wire are shown in **Figure 4A–C** respectively. Plateaus at around 0.75, 1.05, 0.8 and 2.85, 2.65, 2.75 V respectively can be seen. Compared with lithium as an RE (also shown in **Figure S2**, Supporting Information), the relative difference is 2.66 V for LTO, 2.98 V for TiO_2 , and 2.86 V for Ti wire. The GITT-OCP evaluation using an RE enables more accurate representation of the system being evaluated; however, the lengthy transient and relaxation times chosen mean higher susceptibility to electrode drift or instability.

Differential capacities as a function of voltage were analyzed for full pouch cells at 0.2C cycling rate between 2.5 and 4.2 V. **Figure 5** shows that the differential capacity curves can be used for battery ageing evaluation, given that separate anode and cathode values are obtained with the use of REs, enabling analysis of distinct potential curve features.^[32–36] Here it can be observed that the intensity for both the cathode and anode decreases with increase in cycling from the 2nd to 70th cycles. The main feature of the overall cell, cathode, and anode with respect to RE monitoring is the loss of the dQ/dV initial peak 1, which shrinks its initial peak by 40–50%, and the inflexion point between peak 1 and 2 by 10%. In addition, the dQ/dV peaks did not broaden for all cells, which specifies that the kinetics reaction mechanism remains invariant with cycle aging. As such, the reference electrode can identify electrode aging mechanisms by analyzing the

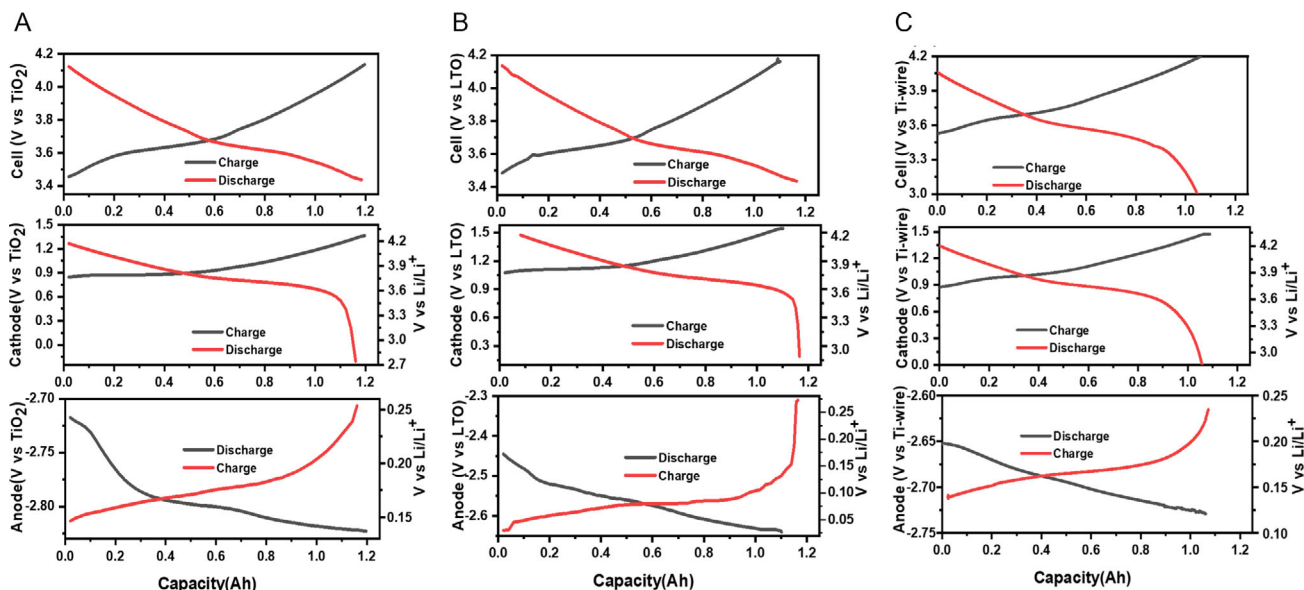


Figure 4. GITT-OCV measurements for the anode, cathode, and full cell of a pouch cell fitted with a RE: A) TiO_2 , B) LTO, and C) Ti wire.

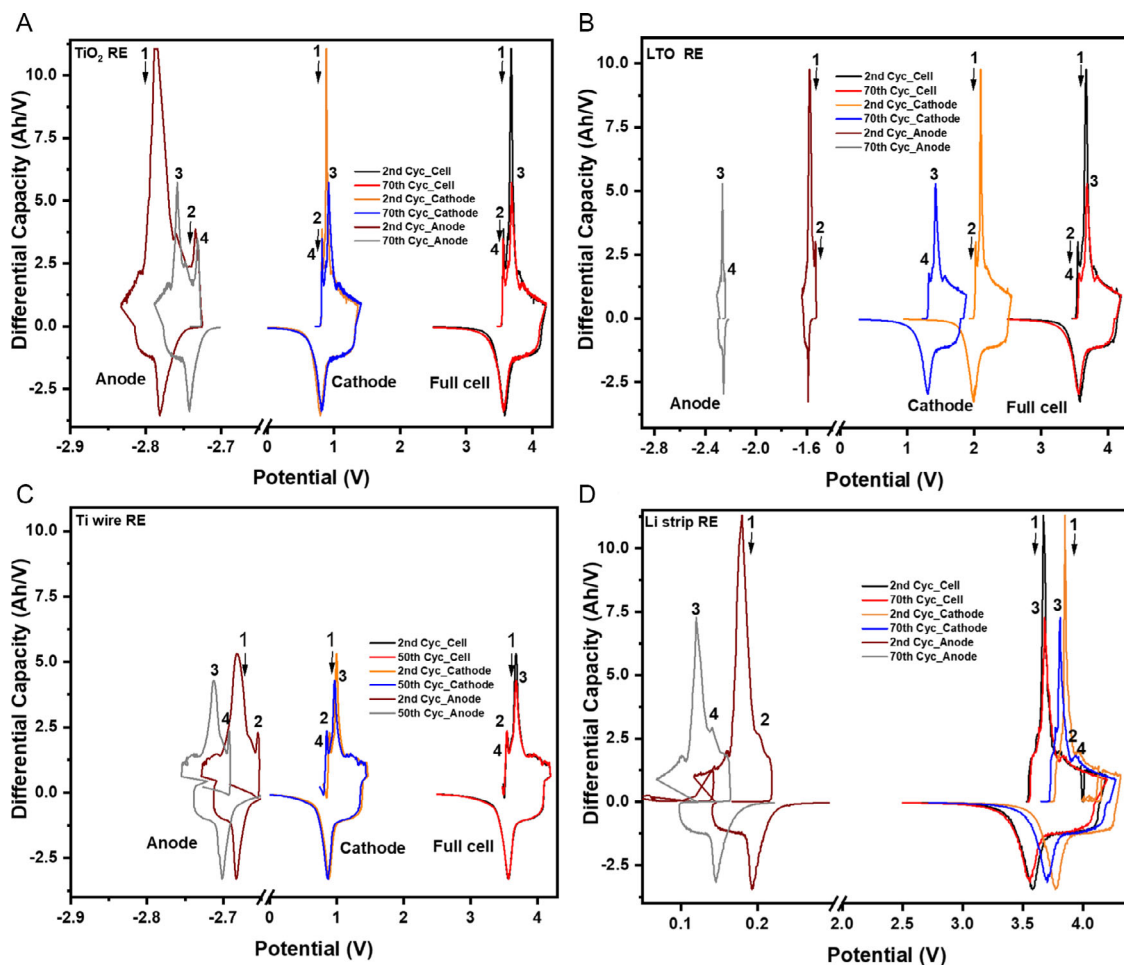


Figure 5. Differential capacity versus electrode voltage of NMC versus graphite positive (NMC) and negative (graphite) half-cells, and extreme right as full cell: A) TiO_2 , B) LTO, C) Ti wire, and D) Li strip.

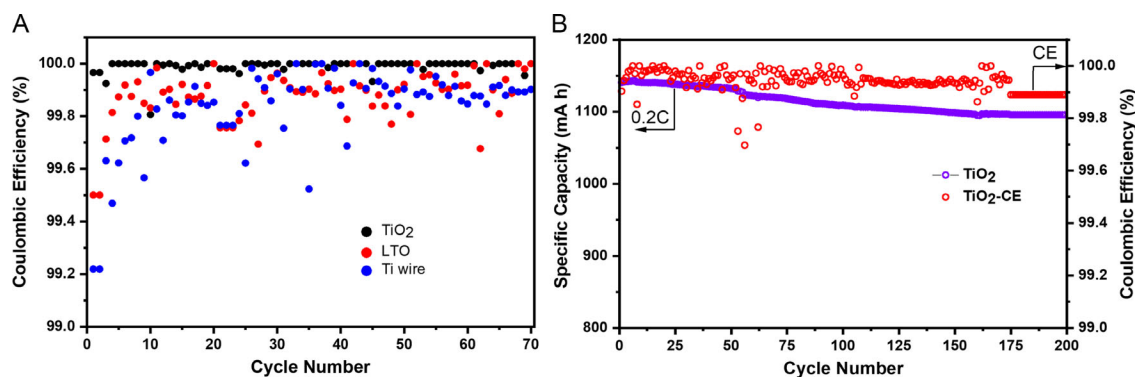


Figure 6. Coulombic efficiency versus cycle number of cells with RE (TiO₂, LTO, and Ti wire) A) for initial 70 cycles at $C/5$ and B) 200 long cycles for RE TiO₂ aged cell with at $C/5$.

changes in each electrode peak that appear with increasing cycle numbers. Finally, there was a significant voltage shift observed in both the cathode and anode of the cell having LTO as an RE at the end of the 70th GCD cycle (as shown in Figure 5B), which could be attributed to the polarization effect.

Coulombic efficiency (CE), defined as specific discharge capacity over the specific charge capacity, was recorded for all cells and is shown in Figure 6. Ti wire shows a comparatively lower CE of around 99.8% compared to LTO and TiO₂ with CE of around 99.9% or higher. The results are displayed in Figure 6A. This could be partially due to the design of the flat-profile REs, while titanium was used in a form of a wire, likely to have a larger impact on the pouch and the sealing process. The electrochemical performance of the aged TiO₂ RE was further assessed through galvanostatic cycling at 0.2C for 200 cycles, as shown in Figure 6B. The Coulombic efficiency was nearly 100% throughout the test.

As noted previously, and for any commercial battery application, high CE and long-term cycling are required, and currently TiO₂ as an RE shows higher CE and prolonged cyclic ability, which can be accredited to stable cell operation despite an additional inserted element. Overall, this demonstrates that such designed REs do not affect the cyclic performance, in favor of adding the functionality of the REs in commercial pouch-cell applications.

4. Conclusion

In this study, we have successfully devised a pouch-cell-insertable, flexible, and miniature RE and used it to evaluate a number of reference electrode materials by integrating into commercially available pouch cells following a standard cell production procedure. Subsequently we used it for characterization techniques and to present its application in the understanding of cathode and anode behavior in a Li-ion battery. The validity and reproducibility of various (Li, Ti, TiO₂, and LTO) reference electrodes was evaluated by several weeks' cycling, and the best among them was TiO₂, exhibiting long-term stability for 1000 h, evaluated over galvanostatic cycles at 0.2C. In addition, we demonstrated the suitability of the TiO₂ RE for potential GCD measurements with subsequent 200 cycles over >2000 h.

The Coulombic efficiency observed during the testing of the cells instrumented this way was stable around 99.9%. This proves the feasibility of implementing the herein-designed REs into pouch cells, a step toward the in-line implementation of REs during cell production. This indicates production compatibility, which might be promising for potential adaptation of this approach on a larger scale.

The GITT and other data obtained were used to define per-electrode GITT-OCP and differential capacity curves, both useful for modeling and aging diagnostics, further reinforcing the usefulness of in situ RE application. Overall, the electrochemical performance measurements showed that long-term cycling stability can be achieved, and identified TiO₂ to be most stable when compared with other Ti-based RE materials. We hope the herein-suggested in situ RE method of integration in full pouch cells will prove useful for further RE material evaluation and subsequently support developing and monitoring advanced systems with improved energy storage characteristics for commercial applications. More work is ongoing on using different in situ RE designs and materials to evaluate various thermal effects on performance, safety, and stability.

Author Contributions

Z.A. and T.A. performed the experiments with the assistance of A.R. All authors wrote the manuscript.

Supporting Information

Supporting Information is available from the Wiley Online Library or from the author.

Acknowledgements

The research work presented in this article was financially supported by the European Union's Horizon 2020 research and innovation project SeNSE (grant agreement No 875548) <https://cordis.europa.eu/project/id/875548> and EPSRC project M-RHEX (EP/R023581/1).

Conflict of Interest

The authors declare no conflict of interest.

Data Availability Statement

The data that support the findings of this study are available from the corresponding author upon reasonable request.

Keywords

battery instrumentation, electrochemistry, lithium-ion batteries, pouch cells, reference electrodes, titanium

Received: July 14, 2021

Published online:

-
- [1] S. Wang, T. Kakumoto, H. Matsui, Y. Matsumura, *Synth. Met.* **1999**, *103*, 2523.
- [2] J. Cannarella, C. B. Arnold, *J. Power Sources* **2014**, *245*, 745.
- [3] R. Raccichini, M. Amores, G. Hinds, *Batteries* **2019**, *5*, 12.
- [4] J. R. Belt, D. M. Bernardi, V. Utgikar, *J. Electrochem. Soc.* **2014**, *161*, A1116.
- [5] G. Nagasubramanian, *J. Power Sources* **2000**, *87*, 226.
- [6] J. Fleming, T. Amietszajew, J. Charmet, A. J. Roberts, D. Greenwood, R. Bhagat, *J. Energy Storage* **2019**, *22*, 36.
- [7] J. Fleming, T. Amietszajew, E. McTurk, D. P. Towers, D. Greenwood, R. Bhagat, *HardwareX* **2018**, *3*, 100.
- [8] T. Amietszajew, J. Fleming, A. J. Roberts, R. Bhagat, W. D. Widanage, D. Greenwood, M. D. Kok, M. Pham, D. J. L. Brett, P. R. Shearing, *Batteries Supercaps* **2019**, *2*, 934.
- [9] E. McTurk, T. Amietszajew, J. Fleming, R. Bhagat, *J. Power Sources* **2018**, *379*, 309.
- [10] S. P. Rangarajan, Y. Barsukov, P. P. Mukherjee, *J. Mater. Chem. A* **2020**, *8*, 13077.
- [11] S. P. Rangarajan, Y. Barsukov, P. P. Mukherjee, *J. Mater. Chem. A* **2019**, *7*, 20683.
- [12] S. P. Rangarajan, Y. Barsukov, P. P. Mukherjee, *J. Electrochem. Soc.* **2019**, *166*, A2131.
- [13] *Handbook of Reference Electrodes*, Vol. 541 (Eds: G. Inzelt, A. Lewenstam, F. Scholz), Springer, Heidelberg **2013**.
- [14] F. La Mantia, C. D. Wessells, H. D. Deshazer, Y. Cui, *Electrochem. Commun.* **2013**, *31*, 141.
- [15] S. Y. Choi, M. Mamak, N. Coombs, N. Chopra, G. A. Ozin, *Adv. Funct. Mater.* **2004**, *14*, 335.
- [16] F. Jonas, B. Lebeau, L. Michelin, C. Carteret, L. Josien, L. Vidal, S. Rigolet, P. Gaudin, J. L. Blin, *Microporous Mesoporous Mater.* **2021**, *315*, 110896.
- [17] K. Cassiers, T. Linssen, M. Mathieu, Y. Q. Bai, H. Y. Zhu, P. Cool, E. F. Vansant, *J. Phys. Chem. B* **2004**, *108*, 3713.
- [18] K. Wang, M. A. Morris, J. D. Holmes, *Chem. Mater.* **2005**, *17*, 1269.
- [19] M. Rashid, A. McGordon, L. Somerville, W. D. Widanage, in *Meeting Abstract, The Electrochemical Society, Philadelphia* **2018**, p. 123.
- [20] J. Charmet, J. Bitterli, O. Sereda, M. Liley, P. Renaud, H. Keppner, *J. Microelectromech. Syst.* **2013**, *22*, 855.
- [21] R. Fu, X. Zhou, H. Fan, D. Blaisdell, A. Jagadale, X. Zhang, R. Xiong, *Energies* **2017**, *10*, 2174.
- [22] Y. Masaki, R. J. Brodd, A. Kozawa, *Lithium-Ion Batteries*, Springer, New York **2009**.
- [23] S. Liu, J. Jiang, W. Shi, Z. Ma, H. Guo, in *IEEE Transportation Electrification Conf. Expo, ITEC Asia-Pacific 2014 – Conf. Proc.*, IEEE, Piscataway, NJ **2014**, pp. 1–3.
- [24] R. Xiong, Y. Pan, W. Shen, H. Li, F. Sun, *Renewable Sustainable Energy Rev.* **2020**, *131*, 110048.
- [25] M. Pfanzelt, Doctoral dissertation, Verlag Nicht Ermittelbar, **2012**.
- [26] N. Alotaibi, Doctoral dissertation, University of Sheffield, **2015**.
- [27] W. H. Ryu, D. H. Nam, Y. S. Ko, R. H. Kim, H. S. Kwon, *Electrochim. Acta* **2012**, *61*, 19.
- [28] G. J. Wang, J. Gao, L. J. Fu, N. H. Zhao, Y. P. Wu, T. Takamura, *J. Power Sources* **2007**, *174*(2), 1109.
- [29] H. K. Kim, S. M. Bak, K. B. Kim, *Electrochem. Commun.* **2010**, *12*, 1768.
- [30] P. Kubiak, M. Pfanzelt, J. Geserick, U. Hörmann, N. Hüsing, U. Kaiser, M. Wohlfahrt-Mehrens, *J. Power Sources* **2009**, *194*, 1099.
- [31] S. B. Patil, H. Phattepur, B. Kishore, R. Viswanatha, G. Nagaraju, *Mater. Renewable Sustainable Energy* **2019**, *8*, 1.
- [32] J. Zhou, P. H. L. Notten, *J. Electrochem. Soc.* **2004**, *151*, A2173.
- [33] S. J. An, J. Li, C. Daniel, S. Kalnaus, Wood, D. L. III, *J. Electrochem. Soc.* **2017**, *164*, A1755.
- [34] P. Jehnichen, K. Wedlich, C. Korte, *Sci. Technol. Adv. Mater.* **2019**, *20*, 1.
- [35] D. Anseán, M. Dubarry, A. Devie, B. Y. Liaw, V. M. García, J. C. Viera, M. González, *J. Power Sources* **2017**, *356*, 36.
- [36] D. Anseán, M. Dubarry, A. Devie, B. Y. Liaw, V. M. García, J. C. Viera, M. González, *J. Power Sources* **2016**, *321*, 201.